Enhancement of irradiation effects on cancer cells by cross-linked dextran-coated iron oxide (CLIO) nanoparticles

Article *in* Physics in Medicine and Biology · January 2010

DOI: 10.1088/0031-9155/55/2/009 · Source: PubMed

IOP PUBLISHING PHYSICS IN MEDICINE AND BIOLOGY

Phys. Med. Biol. **55** (2010) 469–482 doi:10.1088/0031-9155/55/2/009

Enhancement of irradiation effects on cancer cells by cross-linked dextran-coated iron oxide (CLIO) nanoparticles

Fu-Kuo Huang[1], Wen-Chang Chen[1], Sheng-Feng Lai[1], Chi-Jen Liu[2], Cheng-Liang Wang[2], Chang-Hai Wang[2], Hsiang-Hsin Chen[2], Tzu-En Hua[2], Yi-Yun Cheng[2], M K Wu[2], Y Hwu[2,3,4,5], Chung-Shi Yang[6] and G Margaritondo[7]

[1] Department of Chemical and Materials Engineering, National Yunlin University of Science and Technology, 123, University Rd, Sec. 3, Douliu, Yunlin 64002, Taiwan, Republic of China
[2] Institute of Physics, Academia Sinica, Nankang, Taipei 115, Taiwan, Republic of China
[3] Department of Engineering and System Science, National Tsing Hua University, Hsinchu 300, Taiwan, Republic of China
[4] Institute of Optoelectronic Sciences, National Taiwan Ocean University, Keelung 202, Taiwan, Republic of China
[5] National Synchrotron Radiation Research Center, Hsinchu 300, Taiwan, Republic of China
[6] Center for Nanomedicine Research, National Helath Research Institute, Miaoli 350, Taiwan, Republic of China
[7] Ecole Polytechnique Fédérale de Lausanne (EPFL), CH-1015 Lausanne, Switzerland

E-mail: chenwc@yuntech.edu.tw and giorgio.margaritondo@epfl.ch

Received 16 May 2009, in final form 22 November 2009
Published 21 December 2009
Online at stacks.iop.org/PMB/55/469

Abstract

We investigated iron oxide nanoparticles with two different surface modifications, dextran coating and cross-linked dextran coating, showing that their different internalization affects their capability to enhance radiation damage to cancer cells. The internalization was monitored with an ultrahigh resolution transmission x-ray microscope (TXM), indicating that the differences in the particle surface charge play an essential role and dominate the particle–cell interaction. We found that dextran-coated iron oxide nanoparticles cannot be internalized by HeLa and EMT-6 cells without being functionalized with amino groups (the cross-linked dextran coating) that modify the surface potential from −18 mV to 13.4 mV. The amount of cross-linked dextran-coated iron oxide nanoparticles uptaken by cancer cells reached its maximum, 1.33×10^9 per HeLa cell, when the co-culture concentration was 40 μg Fe mL^{-1} or more. Standard tests indicated that these internalized nanoparticles increased the damaging effects of x-ray irradiation, whereas they are by themselves biocompatible. These results could lead to interesting therapy applications; furthermore, iron oxide also produces high contrast for magnetic resonance imaging (MRI) in the diagnosis and therapy stages.

1. Introduction

Each substance used for cancer diagnosis or therapy is affected by biocompatibility and complicated metabolism; therefore, the possibility of using one substance for different tasks (multifunctionality) is particularly attractive. In this context, iron oxide nanoparticles are already quite interesting both as contrast enhancers in magnetic imaging and as drug carriers. Our present results open the possibility of an additional function as enhancers of cancer therapy.

The above function characteristics of the nanoparticle systems are related to the so-called enhanced permeation and retention (EPR) effect (Maeda 2000). We selected iron oxide nanoparticles because of their known contrast enhancement effect in MRI (Lemarchand *et al* 2004, Medarova *et al* 2006, Moore *et al* 2004) and demonstrated that such nanoparticles are good candidates for a multifunctional strategy by also proving their potential therapeutical role. Such a role is specifically based on the enhancement of the effects of radiotherapy, a leading method to fight cancer. The combination of accurate tumor imaging and irradiation effect enhancement could substantially improve the effectiveness of this well-established therapy.

It was previously demonstrated that radiation therapy can be enhanced by introducing into the tumor highly radiation absorbing materials, typically containing high-Z elements (McMahon *et al* 2008). For this objective, various chemicals (Wardman 2007) and nanoparticles (Hainfeld *et al* 2008, 2004, Liu *et al* 2008, McMahon *et al* 2008, Yang *et al* 2008) were used as radiosensitizers. The key problem is to deliver them to the targeted location with sufficient concentration.

The advantages of nanoparticles over more conventional drug delivery systems are their small size (1–100 nm), the ability to evade the immune system (Roeske *et al* 2007) and the high tumor uptake (Hainfeld *et al* 2004, 2008) due to the EPR effect (Maeda 2000). Successful animal tests were performed using gold nanoparticles (Hainfeld *et al* 2004). Gold can also lead to multifunctionality by enhancing the contrast in radiology and tomography.

Iron oxide nanoparticles can play a similar role by providing excellent contrast for MRI even at low concentration (Lemarchand *et al* 2004, Medarova *et al* 2006, Moore *et al* 2004). Although their x-ray absorption is lower than Au nanoparticles, with an absorption enhancement factor of about 1.2 (Roeske *et al* 2007), they can still be effective as a radiosensitizer. Indeed, our investigation found that iron oxide nanoparticles cause a statistically significant enhancement of the damage to tumor cells induced by x-ray irradiation.

Since the main radiation effects in cell killing are damage to DNA and the chemical attack from radiation-generated free radicals, it would be desirable that the nanoparticles be not only concentrated in tumor areas but actually internalized by cancer cells. The EPR effect produces only the preferential concentration in tumor areas; therefore, additional measures must be adopted to achieve internalization.

For this objective, among the many surface modification methods developed for iron oxide nanoparticles (Gupta and Gupta 2005), we specifically adopted the treatment with dextran followed or not by cross-linking with terminal amino groups. The effects were monitored by different microscopy methods. In particular, transmission x-ray microscopy (TXM) with 25 nm lateral resolution detected nanoparticles inside the cells for unsectioned specimens and their precise locations. The two different surface modifications led to opposite cellular uptake results. Large amounts of CLIO NPs (cross-linked iron oxide nanoparticles), up to 1.33×10^9 per cell, were uptaken and internalized near cell nuclei of HeLa cell. This can be attributed to the increase of surface potential that augments the affinity of nanoparticle with cells. By contrast, for nanoparticles without cross-linking, TXM revealed no internalization.

We tested the enhancement of killing by x-ray irradiation for HeLa and EMT-6 cells with internalized CLIO NPs by monitoring their viability. Such nanoparticles clearly reduced the cell survival, validating the hypothesis of multifunctionality of CLIO NPs as nanodrugs and MRI contrast agents.

2. Experimental details

2.1. Synthesis of dextran-coated iron oxide nanoparticles (DCIO NPs) and CLIO NPs

The nanoparticles were synthesized and modified as described by Moore *et al* (2004). DCIO NPs were synthesized first. 50% (w/v) of dextran (T10, Pharmacosmos), 0.29 M $FeCl_3{\cdot}6H_2O$ (1996-01, JT Baker) and 0.145 M $FeCl_2{\cdot}4H_2O$ (2064-01, JT Baker) were dispersed in deionized water with magnetic stirring. The mixture was then titrated to alkaline by adding drops of 29% (w/w) ammonia water (A669 c-212, Fisher scientific) up to pH 10 and heated at 80 °C for 30 min. The resulting black suspension was neutralized with acetic acid. Aggregates were removed by centrifugation for 15 min at 4000 rpm. The DCIO NPs were separated from unbound dextran and unreacted salts by 100 kDa ultrafiltration (Ultracel, Amicon) at $4000\times g$.

The purified DCIO NP solution then was modified with amino groups to synthesize CLIO NPs (Medarova *et al* 2006). 5× volume of 5 M NaOH and 2× volume of epichlorohydrin (ER-0945, TEDIA) were added to the DCIO NP solution with 8 h stirring at room temperature. Then, 8.5× volume of ammonia water (29%) was added for additional overnight reaction. The synthesized CLIO NPs were further purified by 100 kDa ultrafiltration, washed with deionized water and stored at 4 °C. The sizes of the synthesized DCIO and CLIO NPs are about 4.04 nm and 4.18 nm.

2.2. Cell culture

Cell culture media, antibiotics and fetal bovine serum (FBS) were purchased from HyClone (Logan, UT). HeLa cells (CCL-2, ATCC, Rockville, MD) were propagated in a 10 cm (diameter) tissue culture dish in Dulbecco's Modified Eagle Medium (DMEM) supplemented with 10% FBS, 1% penicillin–streptomycin (PS), 0.15% $NaHCO_3$ (Sigma, St Louis, MO) and 1 mM sodium pyruvate (Sigma, St Louis, MO) at 37 °C in a humidified 5% CO_2 atmosphere. EMT-6 cells (CRL-2755, ATCC, Rockville, MD) were cultured on a 10 cm (diameter) tissue culture dish in DMEM/F12 plus 10% FBS, 1% PS, 0.12% $NaHCO_3$ and 0.5 mM sodium pyruvate at 37 °C under 5% CO_2. The cells grew to 80–90% confluence and were detached by trypsin.

2.3. Cell viability assay

The metabolic activity of each well was determined by using a methylthiazoletetrazolium (MTT; Sigma, St Louis, MO) assay; cells were seeded in 24-well plates reaching a volume of 1 mL per well (1–2 × 10^4 cells mL^{-1}). After culturing for 24 h, an additional volume of 10 μL of CLIO NPs was added and the cells were incubated for 4 to 48 h, followed by the addition of 200 μL MTT (the MTT stock solution is 5 mg mL^{-1} in PBS, phosphate buffered saline) for another 4 h culture. After incubation, the medium was removed. 1 mL of DMSO was added and the samples were incubated at 37 °C for 30 min with constant shaking. Optical absorbance was measured at 570 nm using a microplate reader (Elx 800, Bio-tek), and the cell viability so evaluated was expressed as percent relative to untreated control cells.

2.4. Transmission electron microscopy and dark-field optical microscopy analysis

1×10^5 HeLa cells were seeded on a 10 cm (diameter) culture dish. After 24 h, 40 μg Fe mL^{-1} of DCIO or CLIO NPs were added for 24 h co-culture; the cells were trypsinized, centrifuged and washed three times with PBS 5% sucrose. Subsequently, the cells were fixed for 2 h in 2.5% glutaraldehyde and post-fixed for 2 h in 1% osmium tetroxide. Dehydration was achieved by sequential treatments with 25%, 50%, 75%, 95% and 100% ethanol, followed by 100% resin infiltration and embedding. Ultrathin sections prepared by an ultramicrotome were placed on 200 mesh copper grids for TEM (transmission electron microscopy) analysis with a JEM-2100 F JEOL instrument.

For dark-field optical microscopy, 1×10^5 HeLa cells were seeded on a ϕ 3.5 cm petri dish. After 24 h, 40 μg Fe mL^{-1} of DCIO or CLIO NPs were then added for another 24 h co-culture. The cells were then washed with PBS three times and directly observed by a Cytoviva® microscopy system.

2.5. Transmission x-ray microscopy observations

HeLa or EMT-6 cells were seeded and grown on a poly-L-lysine-coated Kapton film (Kapton® Polyimide Film, DuPont) reaching a density of 5×10^3 cells per dish. Specifically, Kapton (2.5×2.5 cm^2) was covered on the ϕ 3.5 cm petri dish, sterilized with 75% ethanol and incubated under laminar flow for 30 min, followed by 0.01% poly-L-lysine (Sigma, St Louis, MO) rinsing for 10 min, washing with deionized H_2O and drying. HeLa or EMT-6 cells were seeded and incubated for 24 h, DCIO and CLIO NPs were then introduced and the incubation continued for 24 h. Afterward, the cells were fixed with 4% paraformaldehyde for 30 min and sequentially washed with 30%, 50%, 70%, 90% and 95% ethanol. Finally, the cells were repeatedly washed with absolute ethanol for three times, and then dried at room temperature. The cell samples so prepared were analyzed at the 32-C-ID TXM beamline (7.9 KeV) of APS (Advanced Photon Source, Argonne National Laboratory) in the USA.

2.6. ζ-potential measurement

DCIO and CLIO NPs were dispersed in sodium chloride solutions (0.001 M), reaching a concentration of 0.1 mg mL^{-1}. The pH was adjusted by HCl or NaOH. The potential measurements were referred to a 0.001 M NaCl solution; the nanoparticles were then studied with a particle size analyzer (90 plus, Brookhaven Instruments Corporation).

2.7. Quantitative analysis of cellular uptake of CLIO NPs

HeLa or EMT-6 cells (2×10^4 cells per well) were seeded in 24 well culture plates. After 24 h, appropriate volumes of various concentrations of CLIO NPs were added. The iron-labeled cells were incubated for another 24 h in a cell culture medium. The iron content of the cells was determined by Inductively Coupled Plasma Optima Optical Emission Spectrometry (ICP-OES; OPTIMA 5100DV, Perkin Elmer). Specifically, the cells were trypsinized with 100 μL trypsin and 200 μL DMEM after 24 h co-culture with CLIO NPs. The cell suspensions were counted and completely digested by exposure to a mixture (2.0 mL) of 37% hydrochloric acid (1.5 mL) and 69% nitric acid (0.5 mL) in an ultrasonic bath for at least 4 h. Then, the volume was increased to 5 mL with deionized H_2O. The quantitative evaluation of CLIO NP uptake in HeLa cells was performed as described by Chithrani *et al* (2006).

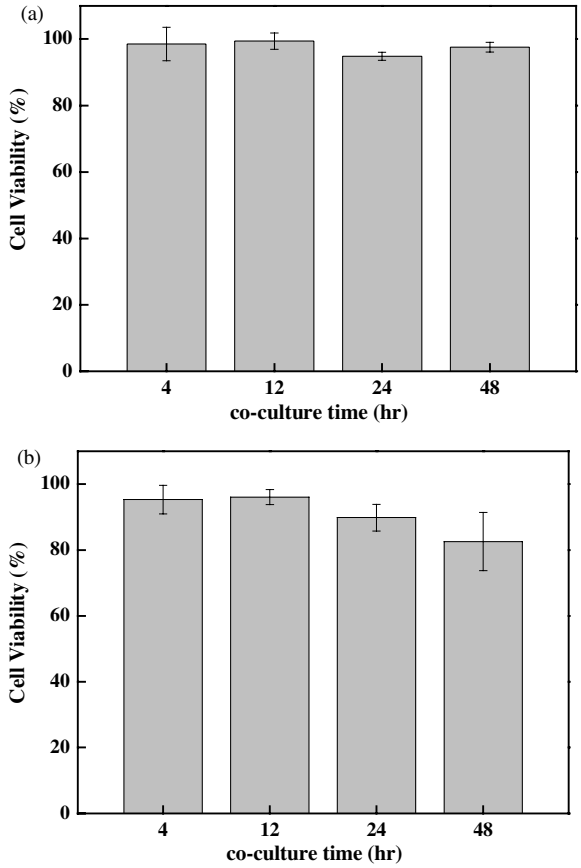

Figure 1. Cell viability assay of HeLa cells co-cultured with 40 μg Fe mL^{-1} of (a) DCIO NPs and (b) CLIO NPs.

2.8. Colongenic cell survival measurements

These measurements were performed with an x-ray Biological Irradiator (RS 2000, Rad Source Technologies, Inc.) operating at 73 keV and with a dose rate of 2.6 Gy min^{-1}. 150 HeLa or EMT-6 cells per well were seeded and grown in a six-well culture dish for 24 h. DCIO or CLIO NPs were then introduced and kept for 24 h more, followed by irradiation with a 0.5, 1, 2, 4, 6, 8 or 10 Gy x-rays dose. The irradiated cells were then further incubated for 14 days. Finally, they were stained with 3% crystal violet and cell colonies were counted (Liu *et al* 2008).

2.9. Statistical analysis

This analysis was performed with the SPSS software package, 12.0 version. The difference with respect to the control specimens was considered as statistically significant when the p-value was <0.05.

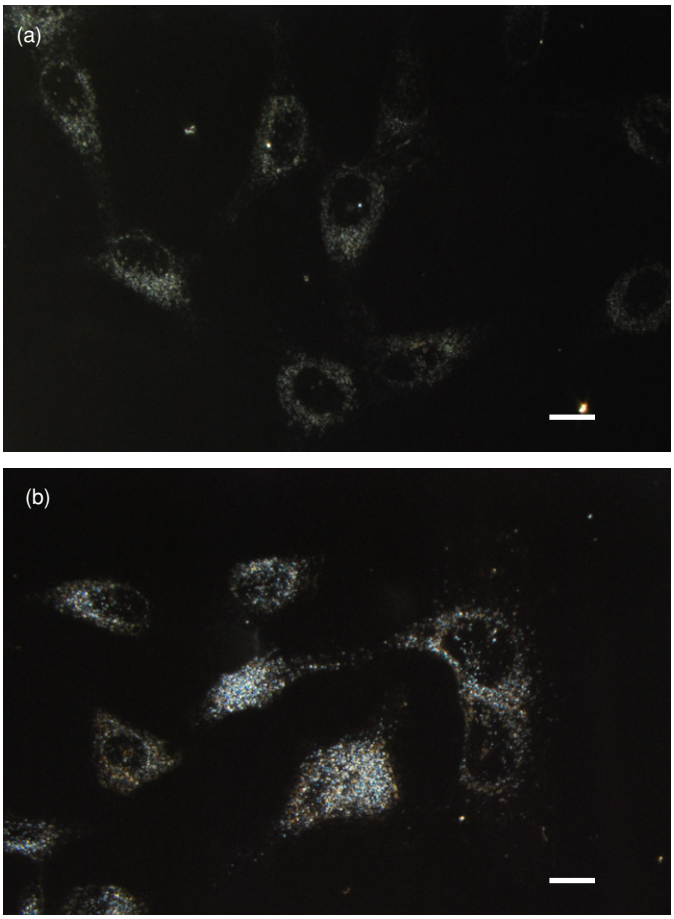

Figure 2. HeLa cells co-cultured with 40 μg Fe mL^{-1} of (a) DCIO and (b) CLIO NPs for 24 h culture and imaged by dark-field optical microscopy. Scale bar: 10 μm.

3. Results and discussions

The HeLa cell cytotoxicity of each type of iron oxide nanoparticles was carefully evaluated for different concentrations and exposure times. The average viability of the control cells determined by the MTT assay was $100 \pm 4.81\%$ for 24 h cultures. The viable percentage for exposure times of 4, 12, 24 and 48 h to DCIO or CLIO NPs (40 μg Fe mL^{-1} concentration) are shown in figure 1. No exposure time effects were observed except for a slight cell viability decrease after 48 h exposure to CLIO NPs. After increasing the CLIO NPs culture concentration to 100 μg Fe mL^{-1}, the HeLa cell viability was still 90%. Our tests overall confirmed previous reports (Song *et al* 2007) that CLIO and DCIO NPs have low cytotoxicity.

The dark-field optical microscopy method is particularly suitable to detect nanoparticles over otherwise transparent backgrounds (Adam and Moy 2005). We used it to monitor the DCIO or CLIO NPs uptake by cells and some results are shown in figure 2. The figures indicate cell internalization of CLIO NPs and no internalization for DCIO NPs.

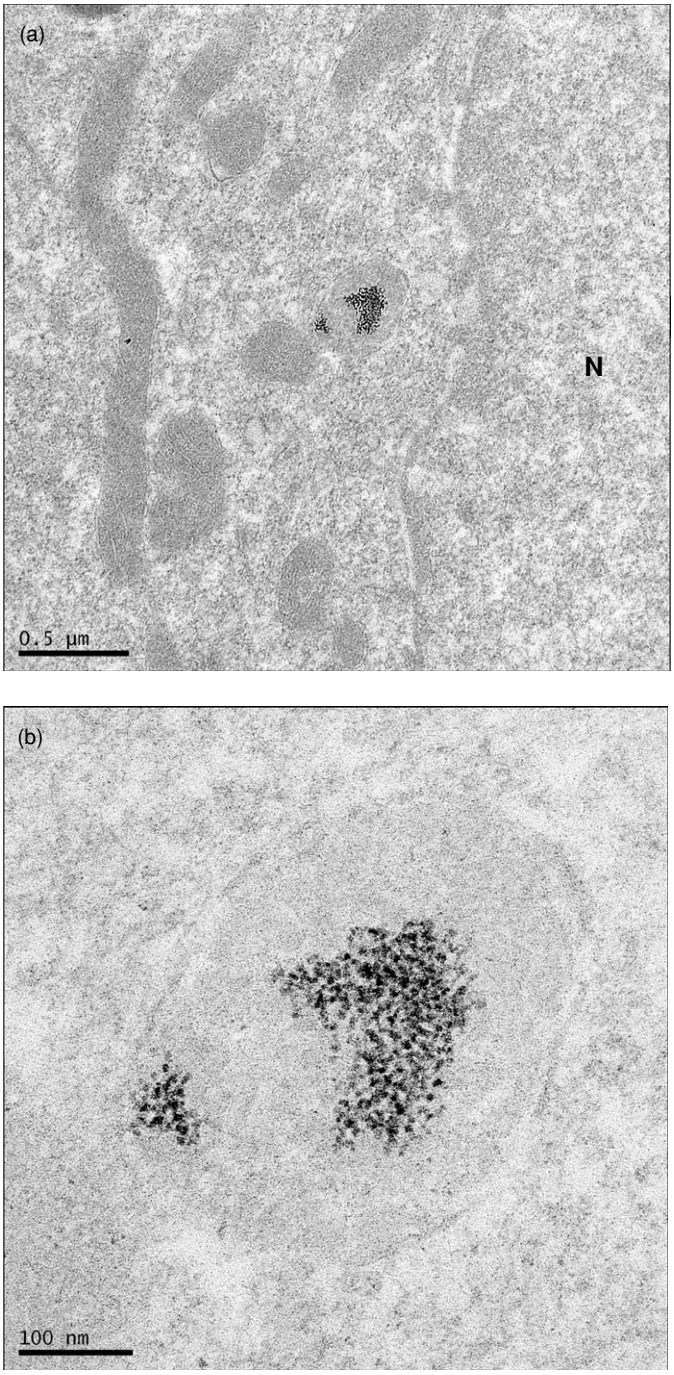

Figure 3. TEM images of the HeLa cell showing the internalization of CLIO NPs. (b) Zoom-in image of part of (a), and note that the CLIO NPs were encapsulated within a vesicle near the cell nucleus (denoted by N).

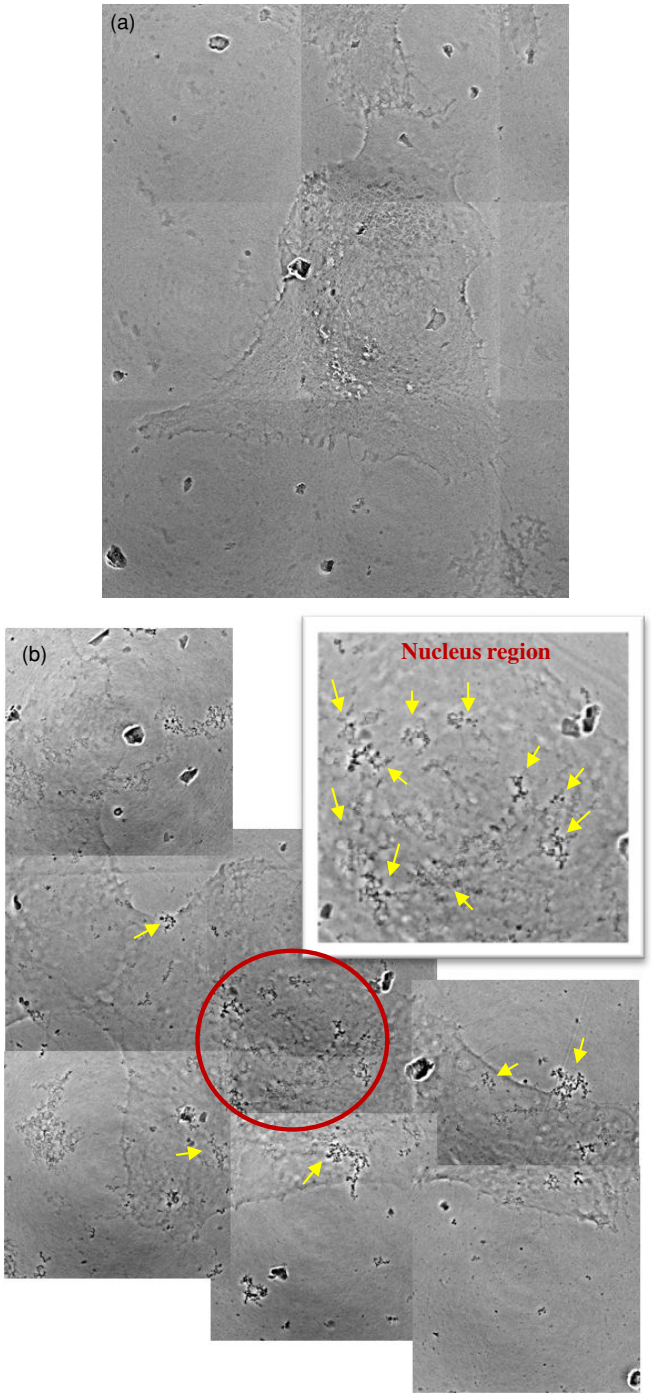

Figure 4. TXM images of (a) DCIO NPs co-cultured with HeLa cells for 24 h at 40 μg Fe mL^{-1}. No nanoparticles are observed inside the cell or on its surface; (b) CLIO NPs co-cultured with HeLa cells for 24 h at 40 μg Fe mL^{-1}. Yellow arrows indicate CLIO nanoparticles; (c) DCIO NPs co-cultured with EMT6 cells for 30 h at 25 μg Fe mL^{-1}; (d) CLIO NPs co-cultured with EMT-6 cells for 30 h at 25 μg Fe mL^{-1}. Yellow arrows indicate CLIO nanoparticles.

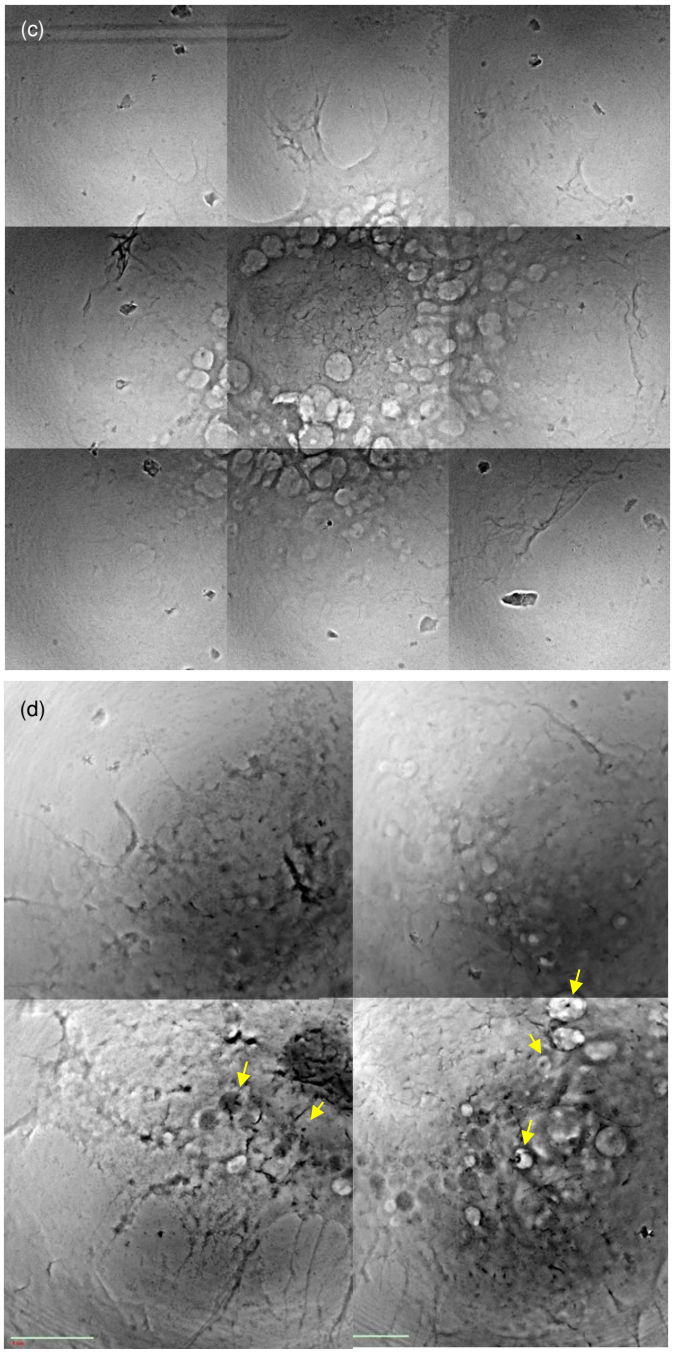

Figure 4. (Continued.)

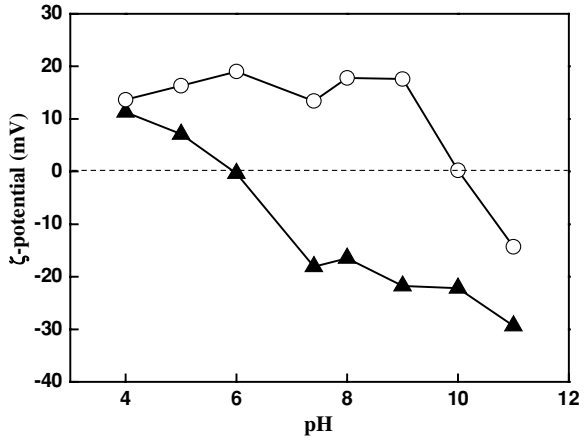

Figure 5. ζ-potential of DCIO (close triangles) and CLIO (open circles) NPs.

Such tests, however, are not conclusive due to the spatial resolution, insufficient to fully guarantee that internalization was indeed achieved. We thus cross-checked them with TEM after sectioning the cell specimens into very thin slices (see figure 3) and TXM. Specifically, TXM with Zernike phase contrast at >8 keV photon energy (Chen *et al* 2008) reaches lateral resolution levels <30 nm sufficient to detect single nanoparticles in subcellular environments (Chu *et al* 2008). As other hard-x-ray imaging techniques (Hwu *et al* 2004), this approach can examine thick biological samples in a relatively natural environment. In this particular work, the cell specimens in figure 3 was only fixed without heavy metal staining which eliminates the possibility of interference of the observation of nanoparticles.

Both TEM and TXM confirmed that CLIO NPs are uptaken by HeLa (and EMT-6) cells, whereas DCIO NPs are not, see the marked NPs in figure 4. Conversely, after examining a large (>300) number of HeLa and EMT-6 cells by TXM, we could conclude that no DCIO NPs were uptaken by, or adhered to, HeLa and EMT-6 cells.

Our present results extend the information on preferential uptake due to surface modification (Song *et al* 2007). For example, TXM (e.g., figure 4) shows that a large numbers of CLIO NPs aggregates are located near nuclei rather than being distributed in the cytosol, an interesting feature in view of possible enhancement of the radiation damage.

The different cellular uptake can be attributed to the different surface potential of DCIO and CLIO NPs (Chung *et al* 2007). The cell surfaces are negatively charged, thus positively charged particles adhere to them, giving way to uptake and internalization. This can be analyzed in terms of ζ-potential measurements for colloidal particles. The results (e.g., figure 5) indicated that the isoelectric point of DCIO and CLIO NPs were at about pH 6 and pH 10. Thus, for a pH of 7.4 the DCIO NPs are negatively charged (-18 mV, not far from the value for uncoated iron oxide nanoparticles), whereas the CLIO NPs are positively charged (13.4 mV).

This difference could be attributed to the amino groups on the CLIO NPs' surface, likely to have polycations-like behavior (Wunderbaldinger *et al* 2002). Indeed, the positive charge of polycations can interact with the negatively charged cell membranes (Unger *et al* 2007) and increase the possibility of translocation across the cell membrane (Mann *et al* 2008). Some concern was expressed (Moghimi *et al* 2005, Slita *et al* 2007, Unger *et al* 2007) about the excessive charge and its possible negative impact of cytotoxicity; in our case, however, no HeLa cell cytotoxicity was detected even when the particles were internalized.

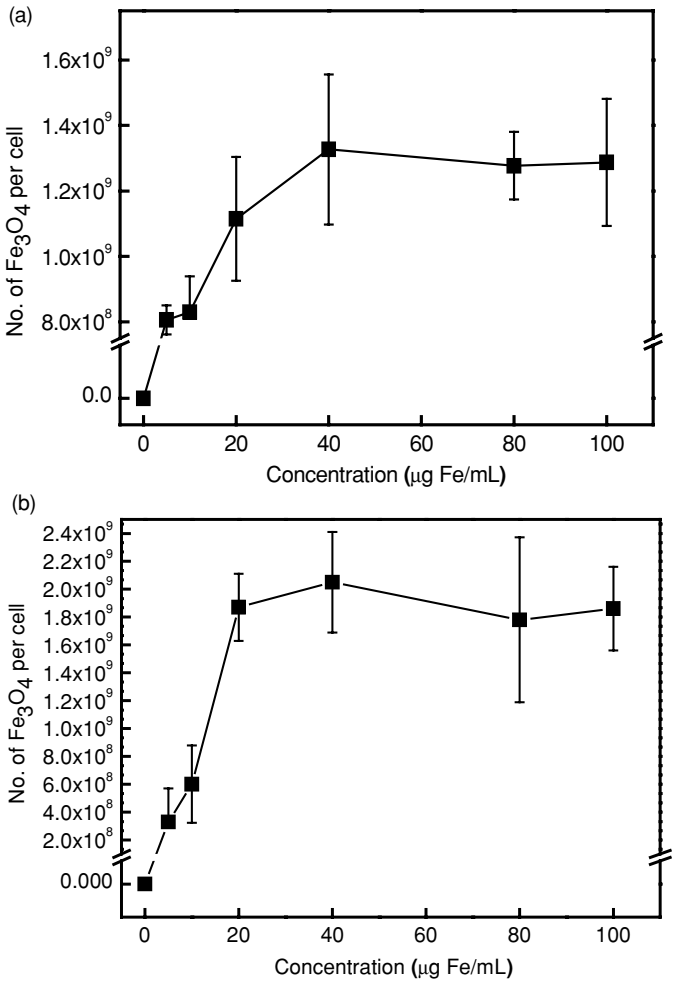

Figure 6. ICP assay of CLIO NPs uptaken by (a) HeLa and (b) EMT-6 cells (24 h co-culture).

The internalization of NPs can be increased by optimizing parameters such as the nanoparticle concentration. The dependence of the cellular uptake on the concentration was measured by ICP. The results (figure 6) showed that the CLIO NP uptake increased up to a maximum level $\sim 1.33 \times 10^9$ per HeLa cell and $\sim 2.05 \times 10^9$ per EMT-6 cell for a concentration of 40 μg Fe mL^{-1} and then saturated. This is reminiscent of the results of Liu *et al* (2008) for x-ray-synthesized Au-PEG nanoparticles, but with a much lower saturation uptake, 5×10^5 per cell; we note, however, that the procedure of Liu *et al* (2008) was not optimized to enhance cell uptake.

We monitored cell viability to assess the effects of internalized CLIO NPs on the killing of cancer cells by x-ray irradiation. The influence of irradiation on cell proliferation was evaluated with long-term (14 days) incubation and the results are shown in figures 7 and 8. CLIO NPs did enhance the x-ray-induced suppression of cell proliferation, whereas DCIO NPs produce no significant effect compared to the control with x-ray irradiation. Note, as already mentioned, both CLIO and DCIO NPs by themselves are biocompatible. Cell damage enhancement was already suggested by the results of a 0.5 Gy x-ray dose, with 76% cell

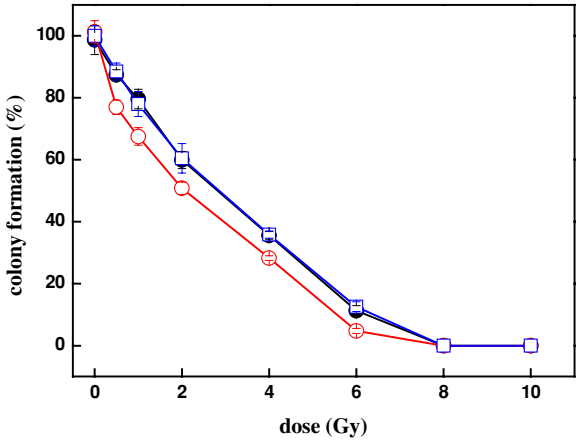

Figure 7. Radiation survival curves of HeLa cells. The full dots are results for HeLa cells cultured for 24 h, whereas the open symbols refer to 24 h exposure to 40 μg Fe mL^{-1} of CLIO NPs (open circles) or DCIO NPs (open square) before and after x-ray irradiation with the indicated dose. The data represent the mean $\pm$ standard deviation of the results from three independent experiments.

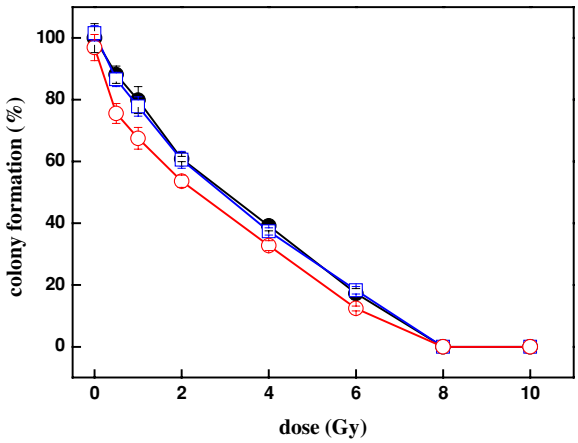

Figure 8. Radiation survival curves of EMT-6 cells. The full dots are results for EMT-6 cells cultured for 24 h, whereas the open symbols refer to 24 h exposure to 40 μg Fe mL^{-1} of CLIO NPs (open circles) or DCIO NPs (open square) before and after x-ray irradiation with the indicated dose. The data represent the mean $\pm$ standard deviation of the results from three independent experiments.

survival rate compared to 89% for the control group. The enhancement became statistically significant for doses between 0.5 and 6 Gy.

The damage enhancement was not simply proportional to the cellular uptake. In the case of HeLa cell, the dose enhancement factor (DEF) estimated from figure 7 is $\sim$1.6 at 1 Gy, $\sim$1.4 at 2 Gy and $\sim$1.33 at 4 Gy, which is far larger than the theoretical calculated value, $<$1.1, of Au nanoparticle at a tissue concentration equivalent to our value of Fe $\sim$0.4 mg g^{-1} (Roeske *et al* 2007). In the case of EMT cell, the DEF estimated from figure 8 is $\sim$1.6 at 1 Gy, $\sim$1.33 at 2 Gy and $\sim$1.14 at 4 Gy. Considering that for the same irradiation condition the DEF of Fe

and Au nanoparticles has a ratio ∼1.2/1.6 (Roeske *et al* 2007), the effect we obtained with our CLIO nanoparticles is thus far stronger than the theoretical evaluations only based on the absorption of the irradiation energy. This is a clear indication that the effect cannot be simply explained as the effect of the increase in x-ray absorption. The underlying mechanisms must thus be clarified by additional investigations.

4. Conclusions

We demonstrated that iron oxide nanoparticles with appropriate surface modifications can dramatically increase the cell internalization and enhance the radiation damage. With the known effect of iron oxide nanoparticles acting as multifunctional nanodrugs with superior specific localization in the tumor via the EPR effect and its magnetic properties for high sensitivity MRI imaging, the additional radiation could lead to potential applications of enhancing radiotherapy. The radiation damage enhancement was specifically observed for uptaken CLIO NPs, whereas for DCIO no uptake was detected. The enhancement was actually observed for two different cell lines, HeLa and EMT-6.

One important point is that CLIO NPs are internalized close to the nucleus. Maximum CLIO NP internalization, 1.33×10^9 per HeLa cell, was obtained above 40 μg Fe mL^{-1} of CLIO NPs in the culture medium. The radiation damage enhancement mechanism is not clear at present, but it cannot be simply attributed to an increase in x-tray absorption.

Acknowledgments

We wish to thank Dr Chia-Fu Chou for the CCD camera setup. This work is supported by the National Science and Technology Program for Nanoscience and Nanotechnology, the Thematic Research Project of Academia Sinica, the Biomedical Nano-Imaging Core Facility at National Synchrotron Radiation Research Center (Taiwan), the Center for Biomedical Imaging (CIBM) in Lausanne, partially funded by the Leenaards and Jeantet foundations the Swiss Fonds National de la Recherche Scientifique and the EPFL.

References

Adam J F and Moy J P 2005 Table-top water window transmission x-ray microscopy: review of the key issues, and conceptual design of an instrument for biology *Rev. Sci. Instrum.* **76** 091301

Chen Y T *et al* 2008 Full-field hard x-ray microscopy below 30 nm: a challenging nanofabrication achievement *Nanotechnology* **19** 395302

Chithrani B D, Ghazani A A and Chan W C W 2006 Determining the size and shape dependence of gold nanoparticle uptake into mammalian cells *Nano Lett.* **6** 662–8

Chu Y S *et al* 2008 Hard-x-ray microscopy with Fresnel zone plates reaches 40 nm Rayleigh resolution *Appl. Phys. Lett.* **92** 103119

Chung T H, Wu S H, Yao M, Lu C W, Lin Y S, Hung Y, Mou C Y, Chen Y C and Huang D M 2007 The effect of surface charge on the uptake and biological function of mesoporous silica nanoparticles 3T3-L1 cells and human mesenchymal stem cells *Biomaterials* **28** 2959–66

Gupta A K and Gupta M 2005 Synthesis and surface engineering of iron oxide nanoparticles for biomedical applications *Biomaterials* **26** 3995–4021

Hainfeld J F, Dilmanian F A, Slatkin D N and Smilowitz H M 2008 Radiotherapy enhancement with gold nanoparticles *J. Pharm. Pharmacol.* **60** 977–85

Hainfeld J F, Slatkin D N and Smilowitz H M 2004 The use of gold nanoparticles to enhance radiotherapy in mice *Phys. Med. Biol.* **49** N309–15

Hwu Y, Tsai W L, Je J H, Seol S K, Kim B, Groso A, Margaritondo G, Lee K H and Seong J K 2004 Synchrotron microangiography with no contrast agent *Phys. Med. Biol.* **49** 501–8

Lemarchand C, Gref R and Couvreur P 2004 Polysaccharide-decorated nanoparticles *Eur. J. Pharm. Biopharm.* **58** 327–41

Liu C J *et al* 2008 Enhanced x-ray irradiation-induced cancer cell damage by gold nanoparticles treated by a new synthesis method of polyethylene glycol modification *Nanotechnology* **19** 295104

Maeda H 2000 The enhanced permeability and retention (EPR) effect in tumor vasculature: the key role of tumor-selective macromolecular drug targeting *Adv. Enzyme Regul.* **41** 189–207

Mann A, Thakur G, Shukla V and Ganguli M 2008 Peptides in DNA delivery: current insights and future directions *Drug Discov. Today* **13** 152–60

McMahon S J, Mendenhall M H, Jain S and Currell F 2008 Radiotherapy in the presence of contrast agents: a general figure of merit and its application to gold nanoparticles *Phys. Med. Biol.* **53** 5635–51

Medarova Z, Pham W, Kim Y, Dai G P and Moore A 2006 *In vivo* imaging of tumor response to therapy using a dual-modality imaging strategy *Int. J. Cancer* **118** 2796–802

Moghimi S M, Symonds P, Murray J C, Hunter A C, Debska G and Szewczyk A 2005 A two-stage poly(ethylenimine)-mediated cytotoxicity: implications for gene transfer/therapy *Mol. Ther.* **11** 990–5

Moore A, Medarova Z, Potthast A and Dai G P 2004 *In vivo* targeting of underglycosylated MUC-1 tumor antigen using a multimodal imaging probe *Cancer Res.* **64** 1821–7

Roeske J C, Nunez L, Hoggarth M, Labay E and Weichselbaum R R 2007 Characterization of the theorectical radiation dose enhancement from nanoparticles *Technol. Cancer Res. Treat.* **6** 395–402

Slita A V, Kasyanenko N A, Nazarova O V, Gavrilova II, Eropkina E M, Sirotkin A K, Smirnova T D, Kiselev O I and Panarin E F 2007 DNA-polycation complexes—effect of polycation structure on physico-chemical and biological properties *J. Biotechnol.* **127** 679–93

Song M, Moon W K, Kim Y, Lim D, Song I C and Yoon B W 2007 Labeling efficacy of superparamagnetic iron oxide nanoparticles to human neural stem cells: comparison of ferumoxides, monocrystalline iron oxide, cross-linked iron oxide (CLIO)-NH_2 and tat-CLIO *Korean J. Radiol.* **8** 365–71

Unger F, Wittmar M and Kissel T 2007 Branched polyesters based on poly[vinyl-3-(dialkylamino)alkylcarbamate-co-vinylacetate-co-vinylalcohol]-graft-poly(D,L-lactide-co-glycolide): effects of polymer structure on cytotoxicity *Biomaterials* **28** 1610–9

Wardman P 2007 Chemical radiosensitizers for use in radiotherapy *Clin. Oncol.* **19** 397–417

Wunderbaldinger P, Josephson L and Weissleder R 2002 Crosslinked iron oxides (CLIO): a new platform for the development of targeted MR contrast agents *Acad. Radiol.* **9** (Suppl. 2) S304–6

Yang W S, Read P W, Mi J, Baisden J M, Reardon K A, Larner J M, Helmke B P and Sheng K 2008 Semiconductor nanoparticles as energy mediators for photosensitizer-enhanced radiotherapy *Int. J. Radiat. Oncol. Biol. Phys.* **72** 633–5